1997-06

UPDATED MEASUREMENTS OF THE ISOTOPIC COMPOSITION OF INTERPLANETARY AND GEOMAGNETICALLY TRAPPED ANOMALOUS COSMIC RAYS

R. A. Leske[1], R. A. Mewaldt[1], A. C. Cummings[1], E. C. Stone[1], and T. T. von Rosenvinge[2]

[1]*California Institute of Technology, Mail Code 220–47, Pasadena, CA 91125, USA*
[2]*NASA / Goddard Space Flight Center, Code 661, Greenbelt, MD 20771, USA*

ABSTRACT

Pure samples of anomalous cosmic rays are measured by *SAMPEX*, both at latitudes where the geomagnetic field acts as a particle rigidity filter, and in the radiation belt of trapped anomalous cosmic rays. We report updated measurements of the isotopic composition of anomalous cosmic ray N, O, and Ne in these two regions, along with isotopic values measured over the poles, and compare our results with those found by previous investigators and with those measured in other samples of solar and galactic material.

INTRODUCTION

Since its launch in July of 1992, the Mass Spectrometer Telescope (MAST) on the *Solar, Anomalous, and Magnetospheric Particle Explorer* (*SAMPEX*) satellite has been collecting data on the energetic particle populations in a low altitude polar Earth orbit. From this orbit, at least three distinct populations of anomalous cosmic ray (ACR) nuclei are accessible, each occupying a different region of the orbit (Leske et al. 1995, 1996). At high invariant latitudes, Λ, over the poles, the mixed population of ACRs and galactic cosmic rays (GCRs) is sampled, with GCRs dominating at high energies and ACRs dominating at the low end of the MAST energy window. At intermediate latitudes ($\sim 50° < \Lambda < 60°$), fully stripped low energy GCRs fall below the local geomagnetic cutoff rigidity and are excluded, while partially charged ACRs of similar energies have a higher rigidity and can penetrate to these latitudes (Mewaldt et al., 1996). At lower invariant latitudes ($< 50°$) is a trapped ACR radi-

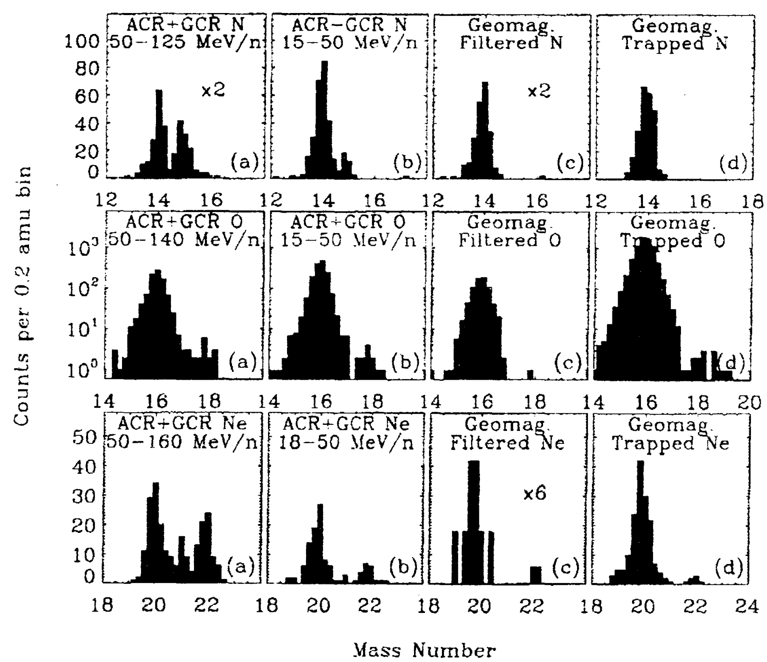

Fig. 1: N, O (note log scales), and Ne mass distributions, including: a) > 50 MeV/nuc GCRs from latitudes $\Lambda > 65°$, b) < 50 MeV/nuc particles (mainly ACRs) from $\Lambda > 65°$, c) geomagnetically filtered, pure ACRs from $\sim 50° < \Lambda < 60°$, and d) ACRs trapped in the magnetosphere ($\Lambda \sim 45°$).

ation belt (Selesnick et al., 1995), with particle intensities $\sim$ 100 times greater than that of ACRs in interplanetary space at 1 AU.

The present measurements differ from our earlier reports on this topic (Leske et al., 1995, 1996) in two important ways. Here we include data through early April of 1997, almost 3 years more data than reported at the previous ICRC (Leske et al., 1995), and about 1.5 years more than included in Leske et al. (1996). Also, we have revised the boundary separating ACRs filtered by the geomagnetic field from those trapped in the ACR radiation belt. Based on the work of Selesnick et al. (1995), we had selected the product $\varepsilon Q = 0.9$ as an upper limit to the trapping boundary, where Q is the ionic charge of the particle and the adiabaticity parameter ε is the ratio of the particle gyroradius to the local scale length of the magnetic field. With the higher statistical accuracy afforded by the present data set, it is now clear that trapped particles extend to higher values of εQ than previously thought, with the difference greatest for Ne (Selesnick et al., 1997). As a result, the statistics for geomagnetically filtered Ne are lower than before, with correspondingly increased statistical uncertainties.

DATA ANALYSIS

Figure 1 shows the mass distributions of N, O, and Ne obtained during solar quiet times in all three latitude intervals of interest here. Panel (a) shows the mass distributions over the poles in the upper portion of the MAST energy interval, while (b) shows the lower energy distribution at the same latitudes. In panel (c) is shown the pure ACR sample obtained at intermediate latitudes, and panel (d) shows the mass distributions in the trapped ACR radiation belt. All events with a tag bit indicating it occurred within $\sim$ 16μs of the previous event have been eliminated, and we restricted the time periods to those in which the instrument trigger rate was $< 15000\ \mathrm{s}^{-1}$. These restrictions help to minimize the degradation in resolution due to trapped proton and alpha particle pileup in the position sensing detectors, as well as intermittent periods of noisy detectors. Since the isotopes of interest are separated by 2 mass units for both oxygen and neon, the trigger rate restriction was not applied for the filtered and trapped Ne and O. This increases the statistics by nearly a factor of 2, while maintaining adequate mass resolution.

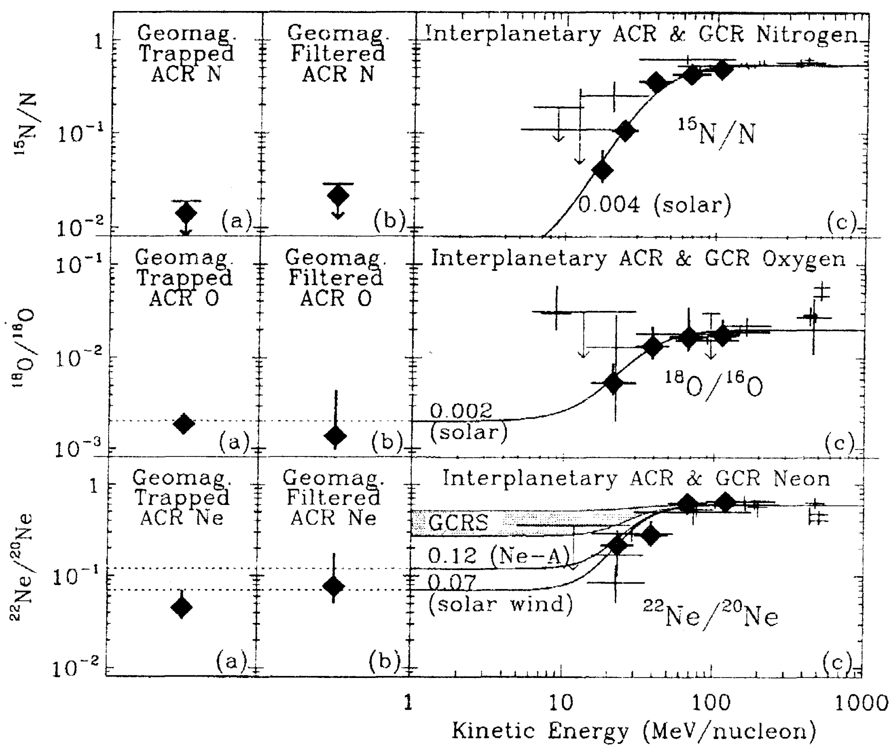

Fig. 2: Measured isotopic abundances for N, O, and Ne from MAST (diamonds), for a) trapped ACRs, b) geomagnetically filtered ACRs, and c) mixed ACRs and GCRs over the poles (plotted vs. energy) compared to previous measurements (plusses; see Leske et al. 1996 for references).

RESULTS

The abundance ratios obtained from these data are listed in Table 1 and plotted in Figure 2, where the high latitude values are compared with those obtained by previous investigators (no prior isotopic measurements exist in the trapped radiation belt or using the geomagnetic filter approach). Curves in Figure 2 are a weighted average of the measured arriving GCR isotopic ratio and an ACR ratio assumed to be either the solar or GCR source value, using energy-dependent weighting factors obtained from power–law fits to the ACR and GCR spectra. Values quoted in Table 1 are the measured ratios, with 1σ uncertainties obtained from a Bayesian treatment of the Poisson statistics.

Table 1: MAST N, O, and Ne Isotopic Composition

Ratio	Location	Energy (MeV/nuc)	Measured Value
^{15}N/N	trapped†	> 15	< 0.0187
^{15}N/N	filtered‡	> 15	< 0.0289
^{15}N/N	$\Lambda > 65°$	15–20	$0.0410(+0.026, -0.011)$
^{15}N/N	$\Lambda > 65°$	20–30	$0.107(+0.035, -0.022)$
^{15}N/N	$\Lambda > 65°$	30–50	$0.356(+0.066, -0.057)$
^{15}N/N	$\Lambda > 65°$	50–90	$0.429(+0.055, -0.052)$
^{15}N/N	$\Lambda > 65°$	90–125	0.492 ± 0.062
^{18}O/^{16}O	trapped†	> 15	$0.00184(+0.00063, -0.00038)$
^{18}O/^{16}O	filtered‡	> 15	$0.00137(+0.00316, -0.00040)$
^{18}O/^{16}O	$\Lambda > 65°$	15–30	$0.0054(+0.0033, -0.0014)$
^{18}O/^{16}O	$\Lambda > 65°$	30–50	$0.0134(+0.0080, -0.0036)$
^{18}O/^{16}O	$\Lambda > 65°$	50–90	$0.0167(+0.0091, -0.0043)$
^{18}O/^{16}O	$\Lambda > 65°$	90–140	$0.0175(+0.0084, -0.0042)$
^{22}Ne/^{20}Ne	trapped†	> 18	$0.045(+0.025, -0.012)$
^{22}Ne/^{20}Ne	filtered‡	> 18	$0.077(+0.103, -0.027)$
^{22}Ne/^{20}Ne	$\Lambda > 65°$	18–30	$0.217(+0.100, -0.057)$
^{22}Ne/^{20}Ne	$\Lambda > 65°$	30–50	$0.282(+0.124, -0.073)$
^{22}Ne/^{20}Ne	$\Lambda > 65°$	50–90	$0.625(+0.185, -0.136)$
^{22}Ne/^{20}Ne	$\Lambda > 65°$	90–160	$0.649(+0.131, -0.105)$

†$\Lambda \sim 45°$;‡ $\sim 50° < \Lambda < 60°$

Table 2: ISM Isotopic Composition from Filtered ACR Measurements

Ratio	Local ISM†	Solar System‡	Local ISM/Solar
^{15}N/N	< 0.029	0.0037	< 8
^{18}O/^{16}O	$0.0014(+0.0033, -0.0004)$	0.0020	$0.69(+1.64, -0.21)$
^{22}Ne/^{20}Ne	$0.079(+0.109, -0.029)$	0.073	$1.08(+1.49, -0.40)$

† Filtered ACR values corrected as in Cummings et al., 1984, 1991

‡ Anders and Grevesse, 1989

At high latitudes, energy dependence is clearly seen in all three isotope ratios, as expected if the ACR isotopic composition differs from that of the arriving GCRs. Deriving the actual ACR composition from this high latitude data is difficult, however, due to the large GCR background even in the lowest MAST energy bin. Taking advantage of the geomagnetic filter approach available in polar Earth orbit eliminates the GCR contamination. Note that the filtered ACR isotope abundances are a factor of ~ 2 lower than the lowest energy ("cleanest") high latitude ACR measurements. Greater statistical accuracy with similarly low background can be achieved using the trapped ACRs. However, deriving ACR abundances from the trapped population requires corrections for any biasing of the mass distribution during the trapping process or during loss from the trapped belt. Such corrections are believed to be of order $\sim$ 10% or less, but are not known in sufficient detail at present to effectively deduce the ACR composition from these data.

Taking the filtered ACRs as most representative of the pure ACR isotopic composition, we apply small corrections of a few percent for mass dependent acceleration and transport effects as in Cummings et al. (1984, 1991), adjusted to measurements at 1 AU at the present phase of the solar cycle. The resulting values for the interstellar medium (ISM) isotopic composition of N, O, and Ne are listed in Table 2, where they are compared with standard solar system values (Anders and Grevesse, 1989).

Due largely to the difficulty in resolving isotopes differing by only one mass unit with a small abundance of one relative to the other, we are only able to report an upper limit on the ^{15}N/N ratio. Our value is still many times the solar value, which in turn is higher than that determined in the local ISM from radio spectroscopy measurements (Wilson and Rood, 1994). It is, however, almost an order of magnitude lower than previously measured values, which were hampered by GCR contamination (Figure 2). Our ^{18}O/^{16}O ratio is consistent with the solar value, as well as the slightly lower value of 0.00179 ± 0.00008 reported in the ISM (Wilson and Rood, 1994). There appears to be no clear consensus on the ^{18}O/^{16}O value at the GCR source, with calculated abundances depending strongly on isotopic production fragmentation cross sections (Guzik et al., 1995).

Our ^{22}Ne/^{20}Ne value for the ISM agrees with the value of $0.077^{+0.068}_{-0.043}$ reported from *Voyager* measurements (Cummings et al., 1991) and with either the solar wind value of 0.073 (Geiss et al., 1972) or the meteoritic component "Ne–A" of 0.12 (Podosek, 1978). It is significantly below the value determined for the GCR source, which is calculated to be somewhere in the range of 0.322 (Connell and Simpson, 1993) to 0.448 (Lukasiak et al., 1994) as indicated (with the reported 1 σ uncertainties) by the shaded band in Figure 2. This indicates that GCRs are not simply an accelerated sample of the ISM (e.g., Olive and Schramm, 1982), but apparently include contributions from sources especially rich in ^{22}Ne, such as Wolf–Rayet stars (Prantzos et al., 1986).

ACKNOWLEDGEMENTS
This work was supported by NASA under contract NAS5-30704 and grant NAGW-1919.

REFERENCES

Anders, E. and Grevesse, N., Geochim. Cosmochim. Acta, 53, 197 (1989).
Connell, J. J. and Simpson, J. A., Proc. 23rd ICRC (Calgary), 1, 559 (1993).
Cummings, A. C., Stone, E. C., and Webber, W. R., ApJL, 287, L99 (1984).
Cummings, A. C., Stone, E. C., and Webber, W. R., Proc. 22nd ICRC (Dublin), 3, 362 (1991).
Geiss, J., Buehler, F., Cerruti, H., et al., Apollo 16 Prelim. Sci. Report, 14–1 (1972).
Guzik, T. G., Albergo, S., Caccia, Z., et al., Proc. 24th ICRC (Rome), 3, 196 (1995).
Leske, R. A., Cummings, A. C., Cummings, J. R., et al., Proc. 24th ICRC (Rome), 2, 606 (1995).
Leske, R. A., Mewaldt, R. A., Cummings, A. C., et al., Space Science Reviews, 78, 149 (1996).
Lukasiak, A., Ferrando, P., McDonald, F. B., and Webber, W. R., ApJ, 426, 366 (1994).
Mewaldt, R. A., Selesnick, R. S., Cummings, J. R., et al., ApJL, 466, L43 (1996).
Olive, K. A. and Schramm, D. N., ApJ, 257, 276 (1982).
Podosek, F. A., Annual Rev. Astron. Astrophys., 16, 293 (1978).
Prantzos, N., Doom, C., Arnould, M., and deLoore, C., ApJ, 304, 695 (1986).
Selesnick, R. S., Cummings, A. C., Cummings, J. R., et al., JGR, 100, 9503 (1995).
Selesnick, R. S., Leske, R. A., Mewaldt, R. A., et al., Proc. 25th ICRC (Durban), this conference, SH 5.4.2 (1997).
Wilson, T. L., and Rood, R. T., Annual Rev. Astron. Astrophys., 32, 191 (1994).